MIT Open Access Articles

THE IMPACT OF STELLAR ROTATION ON THE DETECTABILITY OF HABITABLE PLANETS AROUND M DWARFS

Massachusetts Institute of Technology

THE IMPACT OF STELLAR ROTATION ON THE DETECTABILITY OF HABITABLE PLANETS AROUND M DWARFS

Elisabeth R. Newton[1], Jonathan Irwin[1], David Charbonneau[1], Zachory K. Berta-Thompson[2], and Jason A. Dittmann[1]
[1] Harvard-Smithsonian Center for Astrophysics, 60 Garden Street, Cambridge, MA 02138, USA
[2] Kavli Institute for Astrophysics and Space Research and Department of Physics, Massachusetts Institute of Technology, Cambridge, MA 02139, USA

ABSTRACT

Stellar activity and rotation frustrate the detection of exoplanets through the radial velocity technique. This effect is particularly of concern for M dwarfs, which can remain magnetically active for billions of years. We compile rotation periods for late-type stars and for the M dwarf planet-host sample in order to investigate the rotation periods of older field stars across the main sequence. We show that for stars with masses between 0.25 and 0.5 $M_\odot$ (M4V–M1V), the stellar rotation period typical of field stars coincides with the orbital periods of planets in the habitable zone. This will pose a fundamental challenge to the discovery and characterization of potentially habitable planets around early M dwarfs. Due to the longer rotation periods reached by mid M dwarfs and the shorter orbital period at which the planetary habitable zone is found, stars with masses between 0.1 and 0.25 $M_\odot$ (M6V–M4V) offer better opportunities for the detection of habitable planets via radial velocities.

Key words: stars: low-mass – stars: rotation

1. INTRODUCTION

Radial velocities are a powerful tool for the discovery and characterization of exoplanetary systems. However, stellar magnetic activity and rotation affect the measured radial velocities, as surface inhomegeneities cross the stellar surface and change with time. Starspots diminish light received from the limbs of a rotating star, causing changes in the spectral line centroid (e.g., Saar & Donahue 1997). Plages have a similar influence, but with the opposite sign (e.g., Meunier et al. 2010). Strong localized magnetic fields, typically associated with spots, modify convective flows and cause a net blueshift (e.g., Gray 2009; Meunier et al. 2010). Disentangling these stellar activity signals from the planetary reflex motion is challenging, and typically requires modeling activity-induced changes to spectral line profiles (e.g., Queloz et al. 2009; Boisse et al. 2011; Dumusque et al. 2011, 2012; Rajpaul et al. 2015). This is particularly pertinent for M dwarf stars, which retain high levels of magnetic activity for longer than Sun-like stars. Studies of exoplanets around the nearby M dwarfs Gl 581, Gl 667C, and Gl 191 (Kapteyn's star) have recently highlighted this concern.

Gl 581 is an M3V (Henry et al. 1997)[3] star. Bonfils et al. (2005) first discovered the hot Neptune Gl 581 b orbiting this star, while Udry et al. (2007) identified a second short-period planet, Gl 581 c. The number of additional planets that orbit this star has been a matter of recent debate. Udry et al. (2007) further identified planet d, and Mayor et al. (2009) planet e. Vogt et al. (2010) found evidence for a long-period planet f, and a potentially habitable planet g. Analyses by other groups quickly cast doubt on planets f (Forveille et al. 2011; Tuomi 2011) and g (Gregory 2011; Baluev 2012; Hatzes 2013). Baluev (2012) also raised concerns about planet d. Robertson et al. (2014) looked at the Hα line, a magnetic activity indicator. They found support for the existence of the three innermost planets (b, c, and e), but indications that the outer planets (d, g, and f) are the result of stellar activity and rotation.

Bonfils et al. (2013) identified a super-Earth around Gl 667C, with a second found by Anglada-Escudé et al. (2012b) and Delfosse et al. (2013). Anglada-Escudé et al. (2013b) identified a total of six Keplerian signals at a range of periods. Though long-period signals were seen by Delfosse et al. (2013) and by Makarov & Berghea (2014), they were postulated to be related to the ∼105 day stellar rotation period. Independent analyses by Feroz & Hobson (2013) and Robertson & Mahadevan (2014) did not find evidence for planets exterior to Gl 667C b and c.

Anglada-Escude et al. (2014) reported two planets with periods of 48 and 120 days around Gl 191. Robertson et al. (2015b) showed that the 48 day signal is correlated with stellar activity, and suggested a non-planetary origin. They also express concern that the period of the outer planet is close to the 143 day stellar rotation period.

These examples illustrate that stellar activity signals, which appear at the stellar rotation period and its harmonics, can mimic the effect of a planet at or near these orbital periods. The typical rotation periods of field-age dwarf stars varies by almost an order of magnitude across the lower main sequence, increasing from about 25 days for early G stars (Barnes 2007), to greater than 100 days for mid-to-late M dwarfs (Newton et al. 2016). Over the same stellar mass range, the orbital period corresponding to a habitable planet decreases from approximately 365 days to 10 days. There thus exists a range of stellar masses where the stellar rotation and planetary habitable-zone periods overlap. This came to our team's attention in pursuit of follow-up observations of K2-3, an early M dwarf with three confirmed transiting super-Earths (Crossfield et al. 2015): we noted that the stellar rotation period of ∼40 days is very close to the 44 day orbital period of K2-3 d, which is near the inner edge of the planetary habitable zone.

There are several current and near-future radial velocity surveys committed to finding planets around M dwarf stars, including CARMENES (Quirrenbach et al. 2014), HPF (Mahadevan et al. 2012), and SPIRou (Artigau et al. 2014). It is therefore critical that we understand how stellar rotation may impact the discovery of the potentially habitable planets

---

[3] Included in the RECONS compilation: http://www.recons.org/TOP100.posted.htm.

around these stars. In this Letter, we leverage new rotation periods of mid-to-late M dwarfs in the solar neighborhood from our recent work in Newton et al. (2016) to investigate this problem for stars across the M spectral class.

2. STELLAR ROTATION PERIODS AND MASSES ACROSS THE MAIN SEQUENCE

To assess stellar rotation across the main sequence, we compile literature measurements for the rotation periods of field stars, using data from Baliunas et al. (1996), Kiraga & Stepien (2007), Hartman et al. (2011), Suárez Mascareño et al. (2015), and Newton et al. (2016). The latter supplies most of the rotation period measurements for mid and late M dwarfs, and results from our analysis of photometry from the MEarth-North transit survey (Berta et al. 2012; Irwin et al. 2015). The rotation periods from Hartman et al. (2011) and Kiraga & Stepien (2007) also come from broadband optical or red-optical photometry. On the other hand, Baliunas et al. (1996) and Suárez Mascareño et al. (2015) measure periodicities in chromospheric activity features.

We use stellar mass (M_*) as the independent parameter for this study. For G and early K dwarfs, we use $B - V$ colors to estimate effective temperature (T_{eff}), and then use isochrones to infer M_*. We use the $B - V$ colors provided by Baliunas et al. (1996) and Suárez Mascareño et al. (2015) in their works. We use the empirical relation between $B - V$ color and T_{eff} from Boyajian et al. (2013) to determine T_{eff}. We adopt the 2 Gyr solar-metallicity isochrones from Baraffe et al. (2015).

For late K and M dwarfs, there are known discrepancies between the theoretical and observed stellar temperatures and masses (e.g., Boyajian et al. 2012). For stars with $B - V > 1$, we therefore use the M_K–mass relation from Delfosse et al. (2000), which we have modified to allow extrapolation as described in Newton et al. (2016). Delfosse et al. (2000) calibrated an empirical relation to determine stellar mass by relating the dynamical masses measured from binary orbits to the stars' absolute CIT K magnitudes (M_K). The scatter in the relation is about 10%. We restrict the K and M dwarfs included in this study to those with trigonometric distances. We use NIR magnitudes from 2MASS (Cutri et al. 2003; requiring `qual_flag = AAA`), or alternatively CIT magnitudes from Leggett (1992).

We also include the rotation periods measured from *Kepler* photometry by McQuillan et al. (2014). Most *Kepler* stars do not have parallaxes and they may be subject to interstellar reddening. Therefore, we use the T_{eff} listed in McQuillan et al. (2014). These T_{eff} are adopted from the *Kepler* Input Catalog (KIC; Brown et al. 2011) or, where available, from Dressing & Charbonneau (2013). We then interpolate T_{eff} onto the 2 Gyr solar-metallicity isochrones from Baraffe et al. (2015) to infer stellar mass. The difference in the way masses are estimated for the *Kepler* sample may result in an offset relative to the masses of K and M dwarfs estimated from M_K (e.g., Newton et al. 2015).

Figure 1 shows stellar rotation period as a function of stellar mass for late-type stars in the field. Given the uncertainties in the stellar parameters for the *Kepler* sample, we treat these as an ensemble and plot the distribution instead of the individual measurements. The sensitivity of the McQuillan et al. (2014) analysis may be limited by *Kepler*'s quarterly flux offsets; the other surveys included in this compilation detected periods out to 100 days or longer.

Figure 1 includes stars of a range of ages. As single stars age, they lose angular momentum and their rotation periods increase. Angular momentum loss is mass dependent, with lower-mass stars taking longer to spin down, but eventually reaching longer rotation periods. The long-period envelope of the rotation period distribution is thought to represent an old field population, and the fast rotators at a given mass will eventually evolve toward these long periods.[4] The envelope comprises stars of similar age to the Sun and older, which was established by Skumanich (1972) and Barnes (2003) for Sun-like stars. We quantified this for M dwarfs by using galactic kinematics to estimate that mid M dwarfs with rotation periods around 100 days are on average 5 Gyr old (Newton et al. 2016).
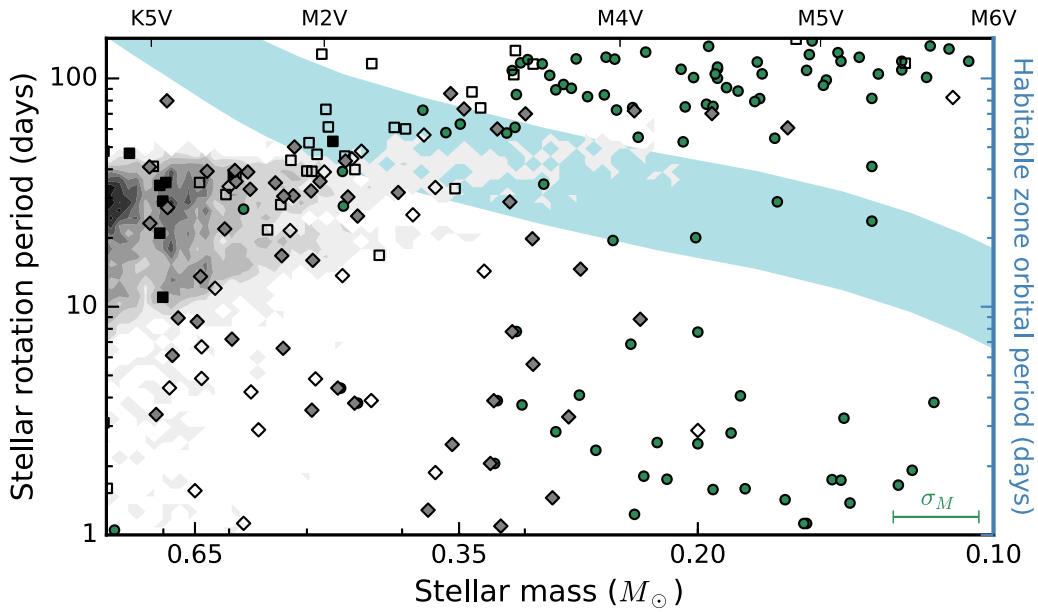
3. STELLAR ROTATION AND THE HABITABLE ZONE

When radial velocity variations induced by stellar rotation and activity coincide with the planetary orbital period, it can be difficult to identify the planetary signal. This stellar signal can appear not just at the rotation period itself, but at higher-order harmonics as well. Boisse et al. (2011) tested cases where the photosphere is dominated by one or two spots and found that power appears primarily at one-half and one-third the stellar rotation period (see also Aigrain et al. 2012). Certain configurations resulted in a low-amplitude signal at one-fourth the rotation period as well. Though spot patterns are likely more complex, both Boisse et al. (2011, 2012) and Aigrain et al. (2012) had success modeling observed radial velocity data. With typical observational sampling, power from these stellar signals leak into nearby frequencies (see, e.g., Figure 15 in Boisse et al. 2011). Thus, stars with rotation periods that are the same as, or two to three times longer than, the habitable zone are not optimal targets for radial velocity searches that aim to discover potentially habitable planets.

The habitable zone from Kopparapu et al. (2013, using values from the erratum) is indicated in Figures 1–3. We adopt the moist greenhouse limit as the inner edge of the habitable zone and the maximum greenhouse as the outer edge of the habitable zone. We use the Baraffe et al. (2015) solar-metallicity 2 Gyr isochrone to calculate T_{eff} and luminosity (L) at a given stellar mass. We note that the choice of stellar models as well as parameters beyond stellar mass, in particular stellar age and metallicity, affect T_{eff} and L, and therefore also the precise location of the calculated habitable zone.

For $0.35\ M_\odot < M_* < 0.5\ M_\odot$, Figure 1 shows that the orbital period of habitable-zone planets is similar to the rotation period of the typical 5 Gyr star. Power can also appear at multiples of the stellar rotation period, so activity signatures can pose problems for habitable-zone planets even with slowly rotating early M dwarfs. This means that stellar rotation can be a confounding factor for $0.25 M_\odot < M_* < 0.5\ M_\odot$. This corresponds to spectral types between M1V and M4V.

We illustrate this idea by considering known M dwarf planet hosts (Figure 2). Our planet-host sample is drawn from the `exoplanet.eu` database (Schneider et al. 2011). We select those stars with $T_{eff} < 4200$ K, $M_* < 0.7\ M_\odot$, $R_* < 0.7\ R_\odot$, and a measured trigonometric parallax. We use the M_K–mass relation from Delfosse et al. (2000) to estimate stellar masses. We use parallaxes from van Leeuwen (2007, from

---

[4] There are handful of early M dwarfs with rotation periods of around 100 days, which stand out as lying above this envelope. Though intriguing, discussion is beyond the scope of this paper.

Figure 1. Stellar rotation period as a function of stellar mass and its relation to the planetary habitable zone. Gray shading shows the rotation period distribution from McQuillan et al. (2014), who analyzed data from *Kepler*. Filled black squares are from Baliunas et al. (1996), and open black squares are from Suárez Mascareño et al. (2015). Open diamonds are from Kiraga & Stepien (2007), and filled diamonds are from Hartman et al. (2011). Green circles are M dwarf rotators from the Newton et al. (2016) statistical sample. The upper envelope indicates the rotation periods of typical, older field stars. The error bar in the lower right indicates the 10% scatter in the empirical M_K–mass relation used to infer stellar mass for the M and and late K dwarfs (Delfosse et al. 2000). The blue shaded region shows the habitable zone as a function of stellar mass from Kopparapu et al. (2013). For early M dwarfs, the habitable-zone period overlaps with the rotation periods of typical stars, both of which are about 40 days. This coincidence complicates the radial velocity detection of habitable planets around early M dwarfs, but not for mid-to-late M dwarfs, or for G and K dwarfs.
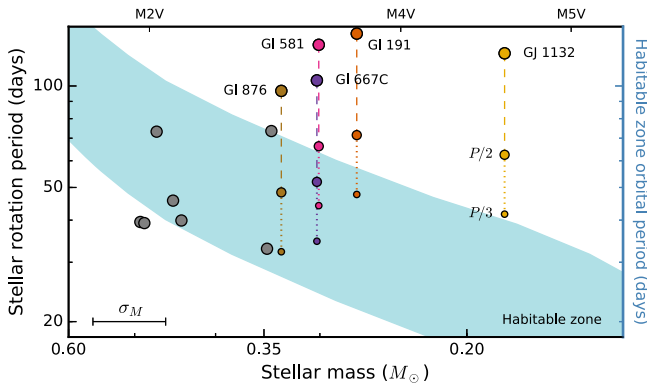
Figure 2. Stellar rotation period vs. stellar mass and its relation to the planetary habitable zone for M dwarfs planet hosts. The error bar in the lower left indicates the 10% scatter in the empirical M_K–mass relation used to infer stellar mass (Delfosse et al. 2000). The blue shaded region shows the habitable zone as a function of stellar mass from Kopparapu et al. (2013). For early M dwarfs, the habitable-zone period overlaps with the rotation periods of typical stars, both of which are about 40 days. GJ 1214 has been excluded from this plot due to the range of published rotation periods (see Table 1).
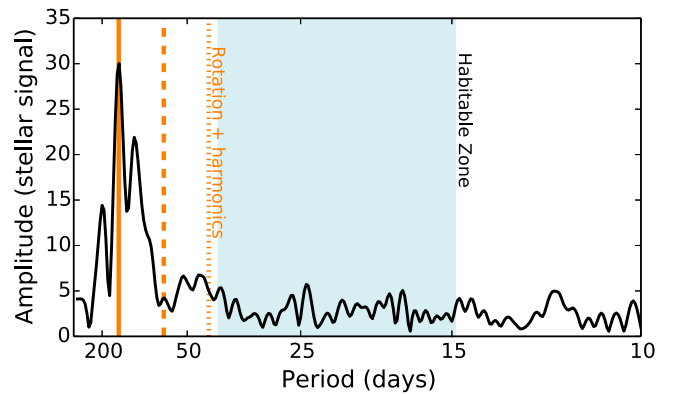
Figure 3. Periodogram of the MEarth light curve for GJ 1132 (Berta-Thompson et al. 2015). The highest peak, indicated by the solid vertical line, is the adopted rotation period. The second and third harmonics are indicated by dashed and dotted lines, respectively; the radial velocity signal from the starspots associated with its photometric variability is expected to have power at these frequencies. The shaded region indicates the planetary habitable zone. The frequency space within which one would find a habitable planet is not expected to be strongly contaminated by stellar activity.

Hipparcos) and supplement with additional sources as necessary. We adopt NIR magnitudes from 2MASS (Cutri et al. 2003, requiring `qual_flag = AAA`). Where 2MASS magnitudes are not available, we use CIT magnitudes from Leggett (1992). We then use the Delfosse et al. (2000) relation to estimate stellar masses and the Boyajian et al. (2012) single-star relation to estimate stellar radii. The Delfosse et al. (2000) relation is based on CIT magnitudes, so we convert 2MASS magnitudes to the CIT system using the relations from Cutri et al. (2006). Stellar rotation periods are compiled from the literature, though many are from Suárez Mascareño et al. (2015). We do not consider estimates from rotational

broadening of spectral lines, which are subject to uncertainty in the inclination angle. These data are listed in Table 1.

Figure 2 shows the rotation periods of these planet hosts. Gl 581, in particular, highlights the challenge early M dwarfs pose for radial velocity surveys seeking to find habitable planets. Though this star has a very long rotation period (130 days), the harmonics dip into the habitable zone. This resulted in the controversy over the potentially habitable planet Gl 581 d ($P_d = 66$ days, at about $P_{rot}/2$), as well as g ($P_g = 36$ days, between $P_{rot}/3$ and $P_{rot}/4$).

GJ 1132 ($M_* = 0.18\ M_\odot$) demonstrates that this is not an issue for many of the lowest-mass M dwarfs. Like many stars

Table 1
Stellar Parameters for M Dwarf Planet Hosts with Trigonometric Parallaxes

Star	Distance (pc)	Ref.[a]	K_S (2MASS)	Mass ($M_\odot$)	Radius ($R_\odot$)	P_{rot} (days)	Ref.[b]
Published Rotation Period							
Gl 176	9.27	vL07	5.607	0.49	0.47	39.5	R15a
Gl 191	3.91	vL07	5.049	0.27	0.28	143.0	R15b
Gl 433	8.88	vL07	5.623	0.47	0.45	73.2	SM15
Gl 436	10.14	vL07	6.073	0.44	0.42	39.9	SM15
Gl 581	6.21	vL07	5.837	0.30	0.30	132.5	SM15
Gl 667C	6.84	vL07	6.036	0.30	0.30	103.9	SM15
Gl 674	4.54	vL07	4.855	0.35	0.34	32.9	SM15
Gl 832	4.95	vL07	4.461	0.45	0.43	45.7	SM15
Gl 849	9.1	vL07	5.594	0.49	0.46	39.2	SM15
Gl 876	4.69	vL07	5.010	0.33	0.33	96.7	R05
GJ 1132	12.04	J05	8.322	0.18	0.21	125.0	BT15
GJ 1214	14.55	AE13	8.782	0.18	0.21	…	(See note)
HIP 57050	11.1	vL07	6.822	0.34	0.34	73.5	H11
No Rotation Period Available							
Gl 15A	3.59	vL07	4.011	0.40	0.39	…	…
Gl 27.1	23.99	vL07	7.394	0.55	0.52	…	…
Gl 163	14.99	vL07	7.135	0.40	0.38	…	…
Gl 179	12.29	vL07	6.942	0.36	0.35	…	…
Gl 180	12.12	vL07	6.598	0.41	0.40	…	…
Gl 229	5.75	vL07	4.131	0.58	0.55	…	…
Gl 317	15.3	AE12	7.028	0.43	0.41	…	…
Gl 328	19.79	vL07	6.352	0.68	0.65	…	…
Gl 422	12.67	vL07	7.035	0.35	0.35	…	…
Gl 649	10.34	vL07	5.624	0.54	0.51	…	…
Gl 682	5.08	vL07	5.606	0.27	0.28	…	…
Gl 687	4.53	vL07	4.501	0.41	0.39	…	…
GJ 3341	23.2	R10	7.733	0.47	0.44	…	…
GJ 3634	19.8	R10	7.470	0.45	0.43	…	…
HIP 12961	23.01	vL07	6.736	0.67	0.64	…	…
HIP 70849	23.57	vL07	6.790	0.67	0.64	…	…
HIP 79431	14.4	vL07	6.589	0.49	0.46	…	…
Wolf 1061	4.29	vL07	5.075	0.30	0.30	…	…

Notes. GJ 1214 displays photometric modulation, but has not yielded a secure rotation period detection. Berta et al. (2011) tentatively derived a rotation period of 52 days from MEarth photometry and noted that the long-period signal in one season of data indicates that the period may be 80–100 days. Our recent re-analysis in Newton et al. (2016) did not yield a firm period detection. Using independent data sets, Narita et al. (2013) and Nascimbeni et al. (2015) found periods of 44 days and approximately 80 days, respectively.
[a] References for trigonometric distances: J05—Jao et al. (2005); vL07—van Leeuwen (2007); R10—Riedel et al. (2010); AE12—Anglada-Escudé et al. (2012a); AE13—Anglada-Escudé et al. (2013a).
[b] References for stellar rotation periods: R05—Rivera et al. (2005); H11—Hartman et al. (2011); R15a—Robertson et al. (2015a); R15b—Robertson et al. (2015b); BT15—Berta-Thompson et al. (2015); SM15—Suárez Mascareño et al. (2015).

of this mass, GJ 1132 has a rotation period ($P_{rot} = 125$ days; Berta-Thompson et al. 2015) comparable to that of Gl 581. We show the periodogram of this data set in Figure 3; there is no significant power at periods shorter than around 60 days. In the photometry, we do not see power at the second and third harmonics, which is not surprising given the near-sinusoidal modulation seen in Berta-Thompson et al. (2015). However, power could still appear at these frequencies in the radial velocities. However, its lower-mass results in shorter periods for potentially habitable planets, and the third harmonic of the stellar rotation period still lies outside the outer edge of the habitable zone (although only barely so).

4. M DWARFS WITH PHOTOMETRIC MONITORING AS TARGETS FOR RADIAL VELOCITY SURVEYS

We have demonstrated that long-period, low-mass rotators provide good targets for radial velocity surveys searching for

habitable planets. We have provided a catalog of stars with detected photometric rotation periods in Newton et al. (2016), which will be useful in selecting such targets. We recommend selecting those targets with long photometric rotation periods (grade A or B rotators, $P \gtrsim 100$ days).

Also of interest to the community will be those stars that may be photometrically quiet. Newton et al. (2016) catalog stars for which we did not detect periodic photometric modulation in the MEarth data. For some of these objects, the light curves were noisy or sparse, which could have prohibited period detection. Further monitoring may indicate whether these stars are good targets for radial velocity surveys. The statistical sample we identified includes the objects more likely to be of immediate interest.

Our statistical sample was the subset of stars for which the number of observations (n_{visits}) and median error (σ) were such that we had good sensitivity to a range of rotation periods

($n_{\mathrm{visits}} > 1200$, $\sigma < 0.005$). Within this sample, we did not detect a periodic signal for 52%. A Kolmogrov–Smirnov test indicates that the distribution of space velocities for the non-detections is statistically indistinguishable from that of the long-period ($P_{\mathrm{rot}} > 70$ days) sample. We infer that, on average, these stars have ages similar to the long-period sample: we generally expect them to be members of the old thin disk and to be slowly rotating. The stars in the statistical sample with no period detections are therefore also promising targets for radial velocity surveys.

5. DISCUSSION

We have demonstrated that the habitable zone of early M dwarfs coincides with the stellar rotation period typical for older field stars (approximately 5 Gyr). Because activity signals are also expected at two and three times the frequency of the stellar rotation, the stars for which this is an issue are those with $0.25 M_{\odot} < M_{*} < 0.5\,M_{\odot}$ (roughly M1V–M4V). This means that stellar activity will be an unavoidable contaminant in radial velocity surveys that are searching for habitable planets around early M dwarfs. Rather than being the exception, we expect that challenges faced in understanding the Gl 581 system are typical for stars with its mass.

The lifetime of stellar activity and of rapid rotation is another important consideration, since precise radial velocity measurements are challenging for stars with strong activity signature and those with rotationally broadened spectral features. West et al. (2008) found that the activity lifetime rises sharply around a spectral type of M4V. Stellar magnetic activity diminishes by 1 Gyr for M0–M3 dwarfs, but may last for 7–8 Gyr for M6–M8 dwarfs. It is approximately 4 Gyr for M4–M5 dwarfs. In what is presumably a related phenomenon, lower-mass stars also retain rapid rotation rates for longer than do higher mass stars: few early M dwarfs are found to be rapidly rotating (McQuillan et al. 2013), while nearly all very late M (and L) dwarfs have detectable rotational broadening Mohanty & Basri (2003). In Newton et al. (2016), we found an abundance of slowly rotating mid M dwarfs (M4V–M6V), and estimated that a rapid loss of angular momentum occurs between 2 and 5 Gyr for mid M dwarfs. These considerations disfavor the latest-type M dwarfs, since strong activity signatures and rapid rotation are expected to persist for a substantial part of the stars' lifetime.

Finally, we consider the prospects for detailed characterization. A key motivation for turning to M dwarfs is that their small stellar size enhances the signals of orbiting planets. However, M dwarfs span nearly a decade in stellar mass and radius. This means that the transit and radial velocity signatures of a planet orbiting a mid-to-late M dwarf are significantly larger than if an analogous planet orbited an early M dwarf. For example, the transit depth of the Earth around the Sun is 0.0084%; for the same size planet orbiting an $R_{*} = 0.5\,R_{\odot}$ star (M1V), the transit depth is 0.034%, while for an $R_{*} = 0.15\,R_{\odot}$ star (M5V), it is 0.37%. Similarly, an Earth-mass planet at the inner edge of the habitable zone induces a radial velocity semi-amplitude of $0.25\,\mathrm{m\,s}^{-1}$ if it orbits an $M_{*} = 0.55\,M_{\odot}$ star (M1V), compared to $0.98\,\mathrm{m\,s}^{-1}$ if it orbits an $M_{*} = 0.15\,M_{\odot}$ star (M5V).

A promising avenue to look for biosignatures on habitable exoplanets is the direct detection of the planetary Doppler shift. Snellen et al. (2013) recently explored the prospects for detecting oxygen by looking at exoplanetary telluric features.

Rodler & López-Morales (2014) undertook a detailed simulation of the feasibility of this detection if using a high-resolution spectrograph on an Extremely Large Telescope. Their work indicates that the detection of oxygen in the atmosphere of a habitable, Earth-sized planet is a significant time investment that will only be feasible for nearby M dwarfs with $M_{*} < 0.25\,M_{\odot}$. This is due to the relative size of the star and the planet, and the orbital periods of planets in the habitable zone. Such a measurement would be within reach only for the nearest and brightest mid-to-late M dwarfs.

We have considered three factors critical to understanding the prospects of detecting and characterizing habitable planets around M dwarfs:

1. The coincidence of the habitable-zone orbital periods and stellar rotation periods.
2. The lifetime of activity and rapid rotation.
3. The accessibility of detailed atmospheric characterization.

We have demonstrated that the confluence of these factors make mid M dwarfs ideal targets for radial velocity surveys that have the goal of discovering habitable planets whose atmospheres can be studied with the *James Webb Space Telescope* and the ELTs. Many of these targets will be discovered in the coming years by radial velocity instruments and transit surveys (the latter of which are likely to receive radial velocity follow-up). Early M dwarfs are tempting targets for such surveys: their relative brightness makes it easier to achieve higher signal-to-noise observations and more precise radial velocity measurements. However, stellar activity signals will be present at the same periods at which the habitable planets are found. Recent debate surrounding the candidate exoplanets orbiting Gl 581, Gl 667C, and Gl 191 have already demonstrated the challenge of disentangling planetary reflex motion from stellar activity signals.

We therefore suggest that radial velocity surveys closely consider the mid M dwarfs, with $0.1 M_{\odot} < M_{*} < 0.25\,M_{\odot}$ (M4V–M6V). Recent work by the MEarth team provides a useful starting place from which to build such a sample in the northern hemisphere. Nutzman & Charbonneau (2008) selected M dwarfs from the Lépine & Shara (2005) northern proper motion catalog with estimated stellar radii $R_{*} < 0.33\,R_{\odot}$ and trigonometric or photometric distances that placed them within 33 pc. We have since obtained low-resolution near-infrared and optical spectroscopy for a quarter of the sample, and astrometric and photometric analysis of the entire MEarth-North data set. The near-infrared spectroscopic survey conducted by Terrien et al. (2015) also includes substantial overlap with the MEarth-North sample, as do the optical spectroscopic surveys from Lépine et al. (2013), Gaidos et al. (2014), and Alonso-Floriano et al. (2015).

Detailed characterization from the MEarth team includes:

1. Kinematic radial velocities (Newton et al. 2014).
2. Spectroscopically estimated stellar parameters (Newton et al. 2015).
3. Hα measurements (West et al. 2015; Newton et al. 2016, in preparation).
4. Trigonometric parallaxes (Dittmann et al. 2014).
5. Optical colors and estimated metallicities (Dittmann et al. 2016).
6. Photometric rotation periods and non-detections (Newton et al. 2016).

REFERENCES

Aigrain, S., Pont, F., & Zucker, S. 2012, MNRAS, 419, 3147
Alonso-Floriano, F. J., Morales, J. C., Caballero, J. A., et al. 2015, A&A, 577, A128
Anglada-Escudé, G., Boss, A. P., Weinberger, A. J., et al. 2012a, ApJ, 746, 37
Anglada-Escudé, G., Rojas-Ayala, B., Boss, A. P., Weinberger, A. J., & Lloyd, J. P. 2013a, A&A, 551, A48
Anglada-Escudé, G., Arriagada, P., Vogt, S. S., et al. 2012b, ApJL, 751, L16
Anglada-Escudé, G., Tuomi, M., Gerlach, E., et al. 2013b, A&A, 556, A126
Anglada-Escude, G., et al. 2014, MNRAS, 443, L89
Artigau, É, Kouach, D., Donati, J.-F., et al. 2014, Proc. SPIE, 9147, 15
Baliunas, S., Sokoloff, D., & Soon, W. 1996, ApJL, 457, L99
Baluev, R. V. 2012, MNRAS, 429, 2052
Baraffe, I., Homeier, D., Allard, F., & Chabrier, G. 2015, A&A, 577, A42
Barnes, S. A. 2003, ApJ, 586, 464
Barnes, S. A. 2007, ApJ, 669, 1167
Berta, Z. K., Charbonneau, D., Bean, J., et al. 2011, ApJ, 736, 12
Berta, Z. K., Irwin, J., Charbonneau, D., Burke, C. J., & Falco, E. E. 2012, AJ, 144, 145
Berta-Thompson, Z. K., Irwin, J., Charbonneau, D., et al. 2015, Natur, 527, 204
Boisse, I., Bonfils, X., & Santos, N. C. 2012, A&A, 545, A109
Boisse, I., Bouchy, F., Hébrard, G., et al. 2011, A&A, 528, A4
Bonfils, X., Delfosse, X., Udry, S., et al. 2013, A&A, 549, A109
Bonfils, X., Forveille, T., Delfosse, X., et al. 2005, A&A, 443, L15
Boyajian, T. S., von Braun, K., van Belle, G., et al. 2012, ApJ, 757, 112
Boyajian, T. S., von Braun, K., van Belle, G., et al. 2013, ApJ, 771, 40
Brown, T. M., Latham, D. W., Everett, M. E., & Esquerdo, G. A. 2011, AJ, 142, 112
Crossfield, I. J. M., Petigura, E., Schlieder, J. E., et al. 2015, ApJ, 804, 10
Cutri, R. M., Skrutskie, F. M., van Dyk, S., et al. 2003, VizieR Online Data Catalog: 2MASS All-Sky Catalog of Point Source, 2246
Cutri, R., Skrutskie, F. M., van Dyk, S., et al. 2006, Explanatory Supplement to the 2MASS All Sky Data Release, http://www.ipac.caltech.edu/2mass/releases/allsky/doc/explsup.html
Delfosse, X., Forveille, T., Ségransan, D., et al. 2000, A&A, 364, 217
Delfosse, X., Bonfils, X., Forveille, T., et al. 2013, A&A, 553, A8
Dittmann, J. A., Irwin, J. M., Charbonneau, D., & Berta-Thompson, Z. K. 2014, ApJ, 784, 156
Dittmann, J. A., Irwin, J. M., Charbonneau, D., & Newton, E. R. 2016, ApJ, in press
Dressing, C. D., & Charbonneau, D. 2013, ApJ, 767, 95

Dumusque, X., Lovis, C., Ségransan, D., et al. 2011, A&A, 535, A55
Dumusque, X., Pepe, F., Lovis, C., et al. 2012, Natur, 491, 207
Feroz, F., & Hobson, M. P. 2013, MNRAS, 437, 3540
Forveille, T., Bonfils, X., Delfosse, X., et al. 2011, A&A, submitted (arXiv:1109.2505)
Gaidos, E., Mann, A. W., Lepine, S., et al. 2014, MNRAS, 443, 2561
Gray, D. F. 2009, ApJ, 697, 1032
Gregory, P. C. 2011, MNRAS, 415, 2523
Hartman, J. D., Bakos, G. Á., Noyes, R. W., et al. 2011, AJ, 141, 166
Hatzes, A. P. 2013, AN, 334, 616
Henry, G. W., Baliunas, S. L., Donahue, R. A., Soon, W. H., & Saar, S. H. 1997, ApJ, 474, 503
Irwin, J. M., Berta-Thompson, Z. K., Charbonneau, D., et al. 2015, in Cambridge Workshop on Cool Stars, Stellar Systems, and the Sun, Vol. 18, ed. G. van Belle, & H. C. Harris. http://www2.lowell.edu/workshops/coolstars18/articles/093-Irwin+_CS18.pdf
Jao, W.-C., Henry, T. J., Subasavage, J. P., et al. 2005, AJ, 129, 1954
Kiraga, M., & Stepien, K. 2007, AcA, 57, 149
Kopparapu, R. K., Ramirez, R., Kasting, J. F., et al. 2013, ApJ, 765, 131
Leggett, S. K. 1992, ApJS, 82, 351
Lépine, S., Hilton, E. J., Mann, A. W., et al. 2013, AJ, 145, 102
Lépine, S., & Shara, M. M. 2005, AJ, 129, 1483
Mahadevan, S., Ramsey, L., Bender, C., et al. 2012, in Ground-based and Airborne Instrumentation for Astronomy IV, Vol. 8446, ed. I. S. McLean, S. K. Ramsay, & H. Takami 84461S
Makarov, V. V., & Berghea, C. 2014, ApJ, 780, 124
Mayor, M., Bonfils, X., Forveille, T., et al. 2009, A&A, 507, 487
McQuillan, A., Aigrain, S., & Mazeh, T. 2013, MNRAS, 432, 1203
McQuillan, A., Mazeh, T., & Aigrain, S. 2014, ApJS, 211, 24
Meunier, N., Desort, M., & Lagrange, A.-M. 2010, A&A, 512, A39
Mohanty, S., & Basri, G. 2003, ApJ, 583, 451
Narita, N., Fukui, A., Ikoma, M., et al. 2013, ApJ, 773, 144
Nascimbeni, V., Mallonn, M., Scandariato, G., et al. 2015, A&A, 579, A113
Newton, E. R., Charbonneau, D., Irwin, J., et al. 2014, AJ, 147, 20
Newton, E. R., Charbonneau, D., Irwin, J., & Mann, A. W. 2015, ApJ, 800, 85
Newton, E. R., Irwin, J., Charbonneau, D., et al. 2016, ApJ, 821, 93
Nutzman, P., & Charbonneau, D. 2008, PASP, 120, 317
Queloz, D., Bouchy, F., Moutou, C., et al. 2009, A&A, 506, 303
Quirrenbach, A., Amado, P. J., Caballero, J. A., et al. 2014, Proc. SPIE, 9147, 91471F
Rajpaul, V., Aigrain, S., Osborne, M. A., Reece, S., & Roberts, S. 2015, MNRAS, 452, 2269
Riedel, A. R., Subasavage, J. P., Finch, C. T., et al. 2010, AJ, 140, 897
Rivera, E. J., Lissauer, J. J., Butler, R. P., et al. 2005, ApJ, 634, 625
Robertson, P., Endl, M., Henry, G. W., et al. 2015a, ApJ, 801, 79
Robertson, P., & Mahadevan, S. 2014, ApJL, 793, L24
Robertson, P., Mahadevan, S., Endl, M., & Roy, A. 2014, Sci, 345, 440
Robertson, P., Roy, A., & Mahadevan, S. 2015b, ApJL, 805, L22
Rodler, F., & López-Morales, M. 2014, ApJ, 781, 54
Saar, S. H., & Donahue, R. A. 1997, ApJ, 485, 319
Schneider, J., Dedieu, C., Le Sidaner, P., Savalle, R., & Zolotukhin, I. 2011, A&A, 532, A79
Skumanich, A. 1972, ApJ, 171, 565
Snellen, I. A. G., de Kok, R. J., le Poole, R., Brogi, M., & Birkby, J. 2013, ApJ, 764, 182
Suárez Mascareño, A., Rebolo, R., González Hernández, J. I., & Esposito, M. 2015, MNRAS, 452, 2745
Terrien, R. C., Mahadevan, S., Deshpande, R., & Bender, C. F. 2015, ApJS, 220, 16
Tuomi, M. 2011, A&A, 528, L5
Udry, S., Bonfils, X., Delfosse, X., et al. 2007, A&A, 469, L43
van Leeuwen, F. 2007, A&A, 474, 653
Vogt, S. S., Butler, R. P., Rivera, E. J., et al. 2010, ApJ, 723, 954
West, A. A., Hawley, S. L., Bochanski, J. J., et al. 2008, AJ, 135, 785
West, A. A., Weisenburger, K. L., Irwin, J., et al. 2015, ApJ, 812, 3